Adsorption 8: 157–163, 2002

Experimental Analysis on the Dynamic Characteristics of a Heat-Regenerative Adsorptive Air-Conditioning System

Y.B. GUI, R.Z. WANG*, J.Y. WU, Y.X. XU AND W. WANG
Institute of Refrigeration and Cryogenics, Shanghai Jiao Tong University, Shanghai 200030, People's Republic of China
rzwang@mail.sjtu.edu.cn

Received April 13, 2001; Revised January 8, 2002; Accepted February 11, 2002

Abstract. Based upon a prototype heat powered heat-regenerative adsorptive air conditioning system, the effects of step times (heat recovery, mass recovery, and half-cycle) on the coefficient of performance (COP) and specific cooling power (SCP) are studied. The characteristics of real thermodynamic cycles and dynamic SCP are also analyzed. Strong dynamic behavior was found in that the COP and SCP varied with step times. It is found in experiment that a long heat-recovery time usually leads to a lower SCP. But both the COP and SCP can be increased 16% and 6%, respectively, if a very short time—0.5 min of mass recovery is initiated before heat-recovery. The appropriate half-cycle time for the prototype is about 20–25 minutes for which the SCP and COP are excellent.

Keywords: adsorption, heat-recovery, air-conditioning, prototype, dynamic characteristics, experiment

1. Introduction

Adsorption is widely used in the fields of separation, purification etc. (Pons, 1998). Recently, due to the serious problem caused by ozone depletion and global warming, the application of adsorption was extended to the refrigeration system, since benign fluids can be used in adsorption refrigeration systems (Meunier, 1999). Compared with traditional refrigeration systems, adsorption systems have additional advantages (Luo and Tondeur, 2000).

Prototype development is a key procedure for commercial application. Various adsorption refrigeration prototypes have been developed. For example, carbon-methanol solar-powered ice maker (Pons and Grenier, 1987), zeolite-water/carbon-methanol cascading heat pump (Douss, 1993), carbon-ammonia convective thermal-wave air-conditioning system (Critoph, 1996), multi-effect complex compound ammonia sorption machines (Vasiliev et al., 1996), thermal-wave heat pump (Miles and Shelton, 1996), and three-stage silica gel-water chiller (Saha et al., 1997) etc. These prototypes can be powered by low-grade thermal sources such as solar energy, natural gas and waste heat (Wang et al., 1999). As predicated (Meunier, 1999), the waste heat adsorptive air conditioning system may be a possible breakthrough.

The term of 'heat-recovery' is popular in the research field of adsorption refrigeration. It means a heat recovery process between the generator and adsorber included. The heating power can be adequately utilized when switching between the generator and adsorber. Such viable combination of recycling waste heat and heat-recovery will make the adsorption refrigeration system more competitive. A waste-heat powered carbon-methanol heat-regenerative adsorptive air-conditioning prototype has been designed and constructed (Gui and Wang, 2001), and many experiments on the prototype have been carried out. This research focuses on half cycle, since both the periodicity of the working parameters and its symmetry relative to half cycle are good in prototype experiment

*To whom correspondence should be addressed.

(Gui et al., 2002). It was found that the step times, such as heat-recovery time, mass-recovery time, and half-cycle time affect the performance greatly. The system shows strong dynamic behaviors.

2. Experimental Prototype

Due to the great influence of the heat capacity of metallic adsorber and thermal fluid on the system performance, a novel adsorber was particularly designed on the premise with less heat capacity ratio (the heat capacity ratio of metallic adsorber and thermal fluid to adsorbent R_{mf} is only 3.11). The cross section is shown in Fig. 1. A prototype of carbon/methanol heat-regenerative adsorptive air-conditioning system was built (shown in Fig. 2) upon this kind of adsorber. In conjunction to Fig. 2, a brief description for the structure and the basic working principle of the air-conditioning system is given as below:

(a) The air-conditioning system consists of two adsorbers, one condenser and one evaporator. An electric heating boiler is used as the heat source for desorption and an inter-cooler for heat rejection from adsorption. Meanwhile, the thermal fluid of both adsorbers are connected to the heating boiler and the inter-cooler respectively through both of the heating and internal cooling fluid circuits responding to the switch of desorption and adsorption. In

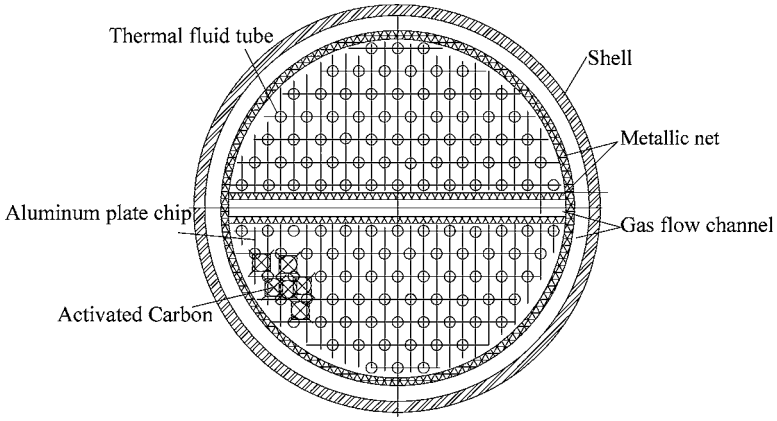

Figure 1. The cross section of a novel adsorber.

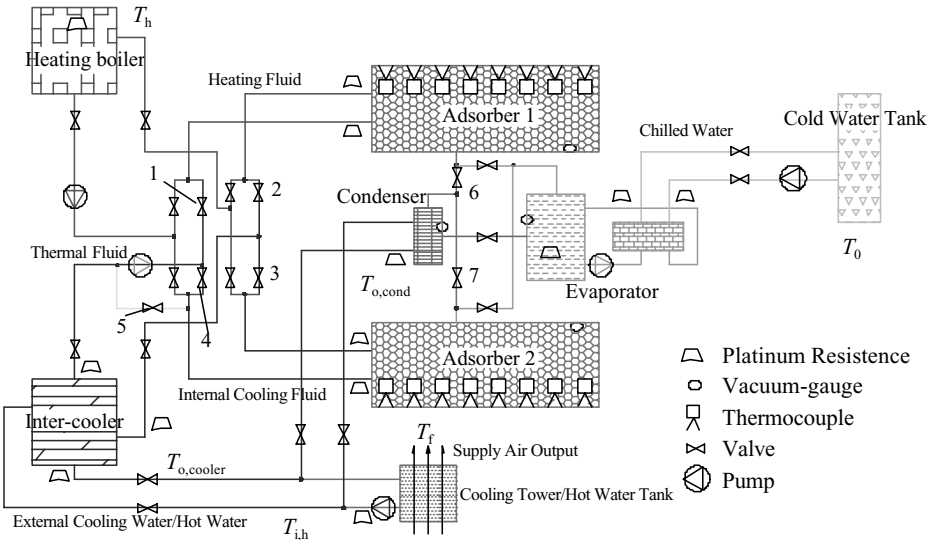

Figure 2. A heat-recovery adsorptive air conditioning prototype.

addition, a cooling tower is used as the heat sink, which receives the heat discharged from the condenser and the inter-cooler. And a cold-water box is used for transferring vaporization heat from air-conditioned room to the evaporator.

(b) Refrigerant vapor desorbed by the generator enters the condenser and turns into saturated refrigerant liquid. It passes through a flow-control valve and reaches the evaporator. Subsequently, saturated refrigerant liquid gasifies in the evaporator motivated by pressure difference between evaporator and adsorber. The continuously supplying of cooling-power mainly depends on continuous adsorption of refrigerant vapor by adsorber, which is guaranteed by the switch between the desorber and adsorber.

3. Heat-Recovery and Mass-Recovery

In the heat recovery process of prototype experiment, heat is recycled from one adsorber to the other when switching them so that the heating power can be adequately used. It can be seen from Fig. 2 that the two adsorbers are in connection by the thermal fluid circuit (the ball valves 1–5 are open in the heat-recovery), and the connection from the two adsorbers to the heating boiler and cooler are blocked (other ball valves are closed). Consequently, the two pumps drive the thermal fluid in the circuit between two adsorbers during this process.

The heat-recovery can be schematically expressed as Fig. 3 in a p-T-x diagram. For example, in the first half cycle, adsorber 2 has provided the recovered heat Q_{rec}

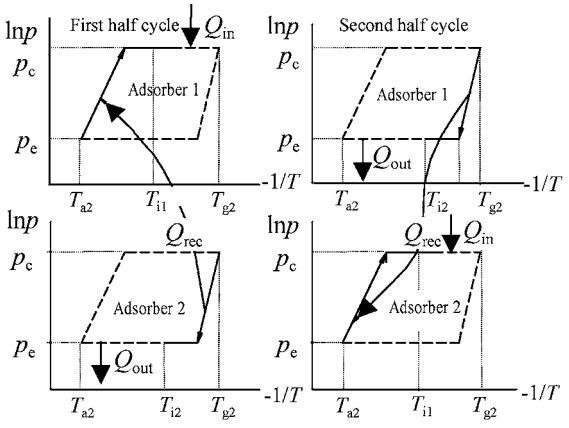

Figure 3. A schematic chart for the heat-recovery system.

for some part of sensible and desorption heat needed by adsorber 1. The energy input Q_{in} from the heating boiler is just needed to meet the demand of the other part of desorption heat of adsorber 1, so heat-recovery is helpful to increase the cycle COP. For an ideal complete heat-recovery, the temperature T_{i2} of the hot adsorber (adsorber 2 in first half cycle) at the end of heat-recovery should be the same as the temperature T_{i1} of the cold one at that time, but it takes too long for the heat-recovery time to improve the performance (see the analysis in Section 6). Consequently, ideal complete heat-recovery is not suitable, usually there should be a temperature difference between T_{i2} and T_{i1} in real cycle.

Mass-recovery could be initiated before heat-recovery. It denotes a particular step in which two adsorbers are simply connected by the refrigerant circuit. As is clear in Figs. 2 and 3, when adsorber 1 (currently as generator) is desorbed, it is at the generation temperature T_{g2} and condensing pressure p_c that is to be cooled to serve as adsorber. While adsorber 2 (currently as adsorber) has adsorbed refrigerant, it is at the adsorption temperature T_{a2} and evaporating pressure p_e that is to be heated to serve as generator at that time. More desorption could be achieved by pressure reduction of adsorber 1, or more adsorption could be obtained if the pressure of adsorber 2 is increased. In this closed adsorption system, the connection between two adsorbers will meet such demands, the two adsorbers pressure will be equalized by the internal mass recovery and will reach an equilibrium pressure close to $p_m = (p_e + p_c)/2$ (Wang, 2001).

From Fig. 2, the operation for the mass-recovery can be easily achieved by the connection of adsorber 1 and adsorber 2 via the solenoid valves 6–7 in the refrigeration circuit (other solenoid valves are closed). A great deal of refrigerant vapor enters into the adsorber 2 from the adsorber 1, so the two adsorbers reach pressure balance very quickly. The mass-recovery process helps to increase the amount of refrigerant in the cycle, due to more desorption in the desorber and also more adsorption in the adsorber (Wang, 2001). Consequently, the refrigeration capacity can be increased. Without additional heat input, this simple process may contribute to increase the system performances, COP and SCP.

In a real system, mass-recovery followed by heat-recovery is very meaningful, and the end of mass-recovery is indicated by pressure balance of the two adsorbers. Thereafter, the pure heat-recovery is in succession. From the analysis of basic working principle

of the prototype, the advantages of the heat-recovery plus mass-recovery processes can be deduced as follows:

(a) Through mass-recovery, the adsorber at the exact adsorption end (future desorber) receives more refrigerant, which will generate more refrigerant to condenser. The adsorber at the exact desorption end (future adsorber) discharges more refrigerant, and will adsorb more refrigerant from evaporator. Consequently, the refrigerant circulation capacity is increased, with the result that the specific cooling power SCP will be increased.
(b) Without mass-recovery, COP increases with the increase of heat-recovery time, while SCP will be reduced. But through mass-recovery, the pressure of the cold adsorber rises quickly. The refrigerant vapor flows into the cold adsorber and is adsorbed, which may cause more heat recovered due to additional adsorption heat, so the effect of heat-recovery is enhanced. It leads to temperature increase of the cold adsorber. At the same time, the temperature of the hot adsorber decreases rapidly because of additional desorption from mass-recovery, so a better COP can be obtained with very short mass-recovery time.

These two virtues of mass-recovery have been validated in the experiments: Under a given set of operating conditions (heat reservoir temperature T_h = 103°C, environment temperature T_o = 24°C, supply-air temperature T_f = 13°C, heat-recovery time t_r = 3 min, half-cycle time t = 15 min), the following performances—COP = 0.244 and SCP = 106 W/kg are obtained for pure heat-recovery. If 0.5 min mass-recovery is added just before heat-recovery, COP = 0.283 and SCP = 113 W/kg are obtained. So the 0.5 min mass-recovery makes COP increase 16% and SCP increase 6% under this condition. As is shown in Fig. 4, the recorded data for these two cycles with and without mass-recovery are quite different in Clapeyron diagram. Obviously, the mass-recovery cycle consists of the process aa' to increase pressure and the process bb' to reduce pressure in Fig. 4, which agrees to the above analyses. But it can also be seen from Fig. 4 that 0.5 min mass-recovery in this occasion is not enough to make the two adsorbers reach pressure equilibrium. Due to the extended cycled adsorptive capacity ΔX (expressed in Fig. 6) (Wang, 2001), the system performance can be improved.

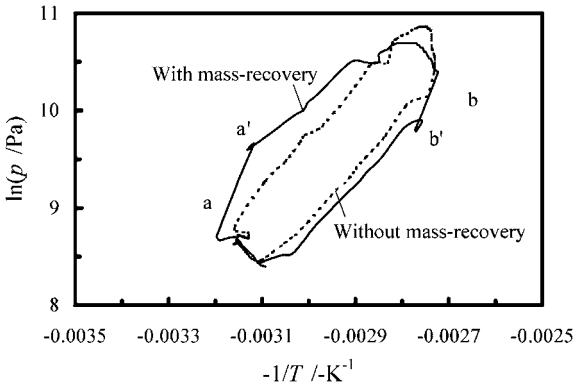

Figure 4. The Clapeyron diagram with and without mass-recovery.

4. Half-Cycle Time

This prototype adopts granule activated-carbon as adsorbent, with the result that the rise and drop rate of adsorber temperature is not very high. So the half-cycle time cannot be too short in real cycle.

On the one hand, with the increase of cycle time, refrigeration effect (kJ) increases due to long adsorption time, but the refrigeration time also increases. Contrarily, the cooling power probably reduces, which leads to a lower SCP. So there is an optimal half-cycle time for the highest SCP.

On the other hand, with the increase of cycle time, COP increases owing to more efficient desorption and adsorption. If heat release to the environment is concerned, long cycle time means consuming more energy in the heating boiler during a long period, which may result in the increase of consuming energy. So there is an optimized cycle time for a maximum COP.

To verify these analyses, prototype experiments are particularly designed under four sets of operating conditions (heat reservoir temperature T_h = 103°C, environment temperature T_o = 26°C, supply-air temperature T_f = 12°C, heat-recovery time t_r = 2 min, half-cycle time t = 12 min/15 min/20 min/25 min). The relation of the system performance versus half-cycle time is obtained, which is shown in Fig. 5.

From Fig. 5, both COP and SCP are small under very short half-cycle time due to small refrigerant circulation capacity caused by insufficient desorption and adsorption. With the increase of half-cycle time, both COP and SCP rise up quickly. SCP reaches a peak value when the half-cycle time is about 20 minutes, and COP reaches the peak value when the half-cycle time is about 25 minutes.

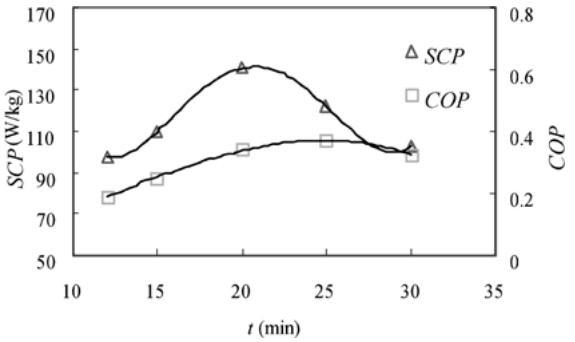

Figure 5. The influence of half-cycle time on COP and SCP.

So under the above experimental conditions, the appropriate half-cycle time for the prototype is about 20–25 minutes when both SCP and COP are excellent.

5. Real Thermodynamic Cycle

Under three sets of operating conditions (heat reservoir temperature $T_h = 103°C$, environment temperature $T_o = 28°C$, supply-air temperature $T_f = 12°C$, heat-recovery time $t_r = 2$ min, cycle time $2t = 30$ min/40 min/60 min), a p-T-X diagram is obtained shown as Fig. 6. This figure shows three real thermodynamic cycles of the above cycle times and also a schematic ideal thermodynamic cycle (heat-recovery cycle). According to Fig. 6, it can be concluded as:

(a) The schematic ideal cycle consists of four processes: isosteric sensible heating—ab, isobaric desorption—bc, isosteric sensible cooling—cd, and isobaric adsorption—da. There are similar four processes in the three real cycles, as is also shown in Fig. 6. To a certain degree, it can be seen that experimental results are consistent with the ideal condition.

(b) Theoretically, the process bc and da are at constant pressure and the process ab and cd are isosteric. It is satisfied that the adsorptive capacity in concentration X_{conc}, the adsorptive capacity in dilution X_{dil} and the condensing pressure p_c of the three real cycles maintain basically stable. But there are some differences between model and experiment. It can be seen that the evaporating pressure p_e in three real cycles fluctuates greatly with temperature.

(c) Obviously, the area enclosed by real cycle curve turns larger when cycle time increases from 30 min to 60 min. The plot of ln p versus $-1/T$ is a way for denoting work. Both the energy consumed in the heating boiler and the cycle refrigeration effect increase with cycle time increasing.

(d) It is well known that the real cycles are non-equilibrium adsorption cycles, though adsorption and desorption process is assumed to have reached equilibrium at different moment of every half cycle in the model (Gui and Wang, 2001). As is shown in Fig. 6, the cycled adsorptive capacity ΔX is extended with the increase of cycle time, which is caused by more adequate adsorption under longer cycle time. It indicates that real cycle becomes closer to steady state under longer cycle time.

6. Dynamic Specific Cooling Power

The terminology—specific cooling power (Gui and Wang, 2001) is defined for a whole cycle. In order

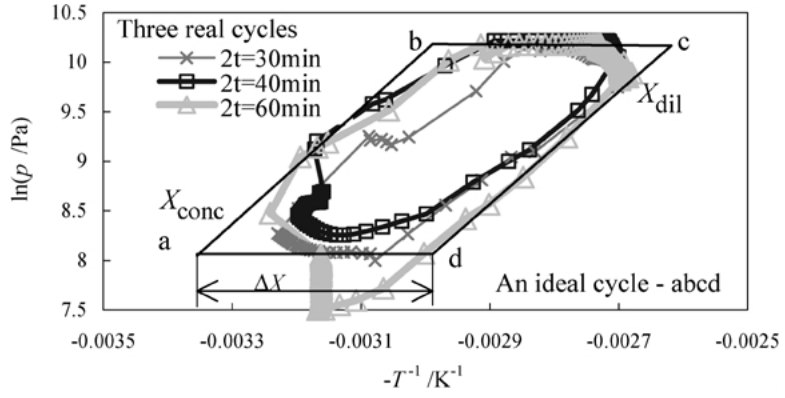

Figure 6. The thermodynamic cycles.

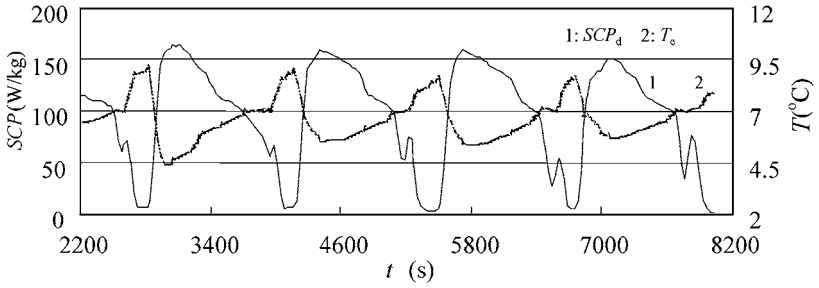

Figure 7. The characteristics of dynamic specific cooling power.

to study the dynamic characteristics of refrigeration during in a cycle, dynamic specific cooling power is defined as:

$$\mathrm{SCP_d} = \frac{m_{\mathrm{ch}} \times c_{\mathrm{ch}} \times \delta T_{\mathrm{ch}}}{M_{\mathrm{c}}} \tag{1}$$

In Eq. (1), M_{c} is mass of activated-carbon adsorbent; m_{ch}, c_{ch} and δT_{ch} are mass flow rate, specific heat capacity and inlet and outlet temperature difference of chilled water respectively.

According to Eq. (1), the characteristic curve of dynamic specific cooling power is obtained from prototype experiment under a set of operating conditions (heat reservoir temperature $T_{\mathrm{h}} = 100°\mathrm{C}$, environment temperature $T_{\mathrm{o}} = 30°\mathrm{C}$, supply-air temperature $T_{\mathrm{f}} = 13°\mathrm{C}$, heat-recovery time $t_{\mathrm{r}} = 3$ min, half-cycle time $t = 20$ min), which is shown in Fig. 7.

Any half cycle in Fig. 7 can be taken for discussion. The beginning of half cycle (the end of heat-recovery) corresponds to the peak value of evaporating temperature T_{e}. At the beginning of half cycle, the adsorption potential between adsorber and evaporator is very strong, which leads to a high vaporization rate in evaporator, so $\mathrm{SCP_d}$ quickly rises to its peak value. But the transferring rate is not high enough for the whole refrigeration effect to export from evaporator; a part of refrigeration effect is consumed to reduce methanol liquid temperature in evaporator, which leads to a quick drop of evaporating temperature T_{e}.

Gradually, adsorption capacity becomes small and adsorption rate becomes slow, so T_{e} rises and $\mathrm{SCP_d}$ drops. Until the beginning of heat-recovery process, the adsorber does not stop adsorbing refrigerant vapor from evaporator. $\mathrm{SCP_d}$ drops a little and T_{e} rises a little at that time, which lead the latish small decrease of T_{e} and the small increase of $\mathrm{SCP_d}$ respectively, because of the function of the heat capacity of evaporator. Thereafter, $\mathrm{SCP_d}$ drops until its minimum, which corresponds to maximum T_{e} (also the end of heat-recovery), and the half cycle ends. Since $\mathrm{SCP_d}$ is relatively small in the whole heat-recovery process, it can be concluded that too long heat-recovery time leads to lower overall SCP.

It is verified by experimental results under two sets of operating conditions (heat reservoir temperature $T_{\mathrm{h}} = 107°\mathrm{C}$, environment temperature $T_{\mathrm{o}} = 33°\mathrm{C}$, supply-air temperature $T_{\mathrm{f}} = 12°\mathrm{C}$, heat-recovery time $t_{\mathrm{r}} = 3$ min/2 min, half-cycle time $t = 15$ min). For the former, $\mathrm{SCP} = 85.6$ W/kg and $\mathrm{COP} = 0.31$ is obtained. For the latter, SCP = 103 W/kg and COP = 0.31 is obtained.

For these two conditions, it is in good agreement with the above analysis that SCP reduces with the increase of heat-recovery time. COP maintains fixed due to short half-cycle time t (equaling 15 min). The consuming power of heating boiler reduces with long heat-recovery time t_{r}, but the cooling power also reduces. Because both reducing amplitudes are almost equivalent in short cycles, COP basically maintains stable. So for a relatively short cycle, heat-recovery time should also be short.

7. Discussion and Conclusion

For consolidated adsorbers or coated surface heat exchanger, SCP value currently approaches 1 kW/kg (Meunier, 1999). Under some experimental conditions on the prototype, SCP is close to 150 W/kg and COP above 0.4 are obtained (Wu et al., 2000). For the use of particle adsorbent, 150 W/kg are still a relatively high value at present. If the thermal fluid (water is presently adopted) in the prototype is replaced by oil, the heat capacity ratio will decrease significantly. Consequently, the performance will be improved, which will be verified on future experiments. In view of the waste heat utilized, the potential application of waste-heat powered heat-regenerative adsorptive air-conditioning system will be great.

From the experimental analysis on the dynamic characteristics of the heat-regenerative adsorptive air-conditioning prototype, some conclusions are drawn as follows.

(a) Combining mass-recovery with heat-recovery increases the SCP.
(b) The appropriate half-cycle time for the prototype is about 20–25 minutes under certain experimental conditions.
(c) Real thermodynamic cycles for heat-regenerative adsorptive air conditioning consist of four-steps, as do the ideal counterparts.
(d) Dynamic SCP is relatively small in overall heat-recovery process, so a long heat-recovery time leads to lower SCP.

Nomenclature

M	Mass (kg)
t	Half-cycle time (min)
t_r	Heat-recovery time (min)
c	Specific heat capacity (J $kg^{-1}{}^{\circ}C^{-1}$)
COP	Coefficient of performance
SCP	Specific cooling power (W/kg)
m	Flow rate (kg/s)
R	Heat capacity ratio
X	Adsorption capacities (kg/kg)
Q_{in}	Energy input from heating boiler (J)
Q_{out}	Heat dissipation via inter-cooler (J)
Q_{rec}	Heat recovered (J)
T	Temperature (°C)
T_{g2}	Generation temperature (°C)
T_{a2}	Adsorption temperatures (°C)
T_{i1}	Cold adsorber temperature at the end of heat-recovery (°C)
T_{i2}	Hot adsorber temperature at the end of heat-recovery (°C)
δ_T	Temperature difference (°C)
p	Pressure (Pa)
p_c	Condensing pressure (Pa)
p_e	Evaporating pressure (Pa)

Subscripts

c	Activated carbon adsorbent
h	Heat reservoir
f	Supply-air from fan-coil
0	Environment
ch	Chilled water
d	Dynamic
e	Evaporator
conc	Concentrated
dil	Dilution
mf	Metallic adsorber and thermal fluid to adsorbent

Acknowledgments

This work was supported by the State Key Fundamental Research Program under the contract No. G2000026309. It is also appreciated for the Teaching and Research Award Program for Outstanding Young Teachers in High Education Institutions of MOE, China.

References

Critoph, R.E., "Gas Fired Air Conditioning Using a Carbon-Ammonia Convective Thermal Wave Cycle," in *Proceedings of International Absorption Conference*, Montreal, pp. 353–360, 1996.

Douss, N., "Experimental Study of Adsorption Heat Pumps Cycles," *International Chemical Engineering*, **33**(2), 207–214 (1993).

Gui, Y.B. and R.Z. Wang, "Practical Three-Heat-Reservoir Model on Heat-Regenerative Adsorption Air-Conditioning System," *Applied Thermal Engineering*, **21**(16), 1643–1656 (2001).

Gui, Y.B., R.Z. Wang, W. Wang, J.Y. Wu, and Y.X. Xu, "Performance Modeling and testing on a Heat-Regenerative Adsorptive Reversible Heat Pump," *Applied Thermal Engineering*, **22**(3), 309–320 (2002).

Luo, L. and D. Tondeur, "Transient Thermal Study of an Adsorption Refrigerating Machine," *Adsorption*, **6**, 93–104 (2000).

Meunier, F., "Adsorption Heat Pump Technology: Possibilities and Limits," in *Proceedings of International Sorption Heat Pump Conference*, Munich, pp. 25–35, 1999.

Miles, D.J. and S.V. Shelton, "Design and Testing of a Solid-Sorption Heat-Pump System," *Applied Thermal Engineering*, **16**(5), 389–394 (1996).

Pons, M., "Full Analysis of Internal Adsorbate Redistribution in Regenerative Adsorption Cycles," *Adsorption*, **4**, 299–311 (1998).

Pons, M. and Ph. Grenier, "Experimental Data on a Solar-Power Ice Maker Using Activated Carbon and Methanol Adsorption Pair," *ASME J. Solar Energy Engineering*, **109**, 303–309 (1987).

Saha, B.B., A. Akisawa, and T. Kashiwagi, "Silica Gel Water Advanced Adsorption Refrigeration Cycle," *Energy*, **22**(4), 437–447 (1997).

Vasiliev, L.L., L.E. Kanonchik, A.A. Kulakov, and A.G. Antuh, "Na_x Zeolite, Carbon Fibre and $CaCl_2$ Ammonia Reactors for Heat Pumps and Refrigerators," *Adsorption*, **2**(4), 311–316 (1996).

Wang, L.J., D.S. Zhu, and Y.K. Tang, "Heat Transfer Enhancement of the Adsorber of an Adsorption Heat Pump," *Adsorption*, **5**, 279–286 (1999).

Wang, R.Z., "Performance Improvement of Adsorption Cooling by Heat and Mass Recovery Operation," *International Journal of Refrigeration*, **24**, 602–611 (2001).

Wu, J.Y., R.Z. Wang, and Y.X. Xu, "Dynamic Simulation and Experiments of a Heat Regenerative Adsorption Heat Pump," *Energy Conversion and Management*, **41**, 1007–1018 (2000).